

# Advancements in the Development of a Novel Wing Design Method in Conceptual Aircraft Design

Tim Effing <sup>\*,†</sup>, Paul Mauerer <sup>\*</sup> and Eike Stumpf <sup>\*</sup>

<sup>\*</sup>Institute of Aerospace Systems, RWTH Aachen University  
Wüllnerstr. 7, 52062, Aachen, Germany

tim.effing@ilr.rwth-aachen.de

<sup>†</sup>Corresponding author

## Abstract

Recently, we presented a novel conceptual wing design method, which uses comprehensive aerodynamic airfoil information to automatically select the most suitable airfoil-sweep combinations for given input data and design objectives. In this work, we present advancements to the design method, more specifically the improvement of the existing design process and the additional consideration of variable camber technology as a driving design factor. The results demonstrate that the method responds comprehensibly to the changes made. However, the additional consideration of variable camber increases the runtime significantly. The actual benefit of the advancements will be evaluated on the overall aircraft design level in future studies.

## 1. Introduction

In the conceptual design of conventional passenger aircraft, the main objective is to derive optimized aircraft configurations capable of fulfilling a predefined set of top-level aircraft requirements. This phase allows the evaluation of aircraft configurations and novel technologies and the rapid exploration of sensitivities for selected key parameters. Due to the complex and multidisciplinary nature of aircraft design, integrated design environments must capture the interdependencies among different design disciplines. One notable characteristic of such conceptual design environments is the requirement for low computational time, even on standard desktop computers. Therefore, simple handbook methods that can effectively reproduce general aircraft characteristics exhibited by the existing fleet are often employed. Promising configurations and integrated technologies are optimized further in later design stages using high-fidelity methods, experimental validation, and flight tests. However, from the initial stages, more advanced methods and detailed information are necessary to fully explore the true potential of an aircraft, particularly when assessing innovative technologies [1]. Recognizing the lack of suitable methods, we recently presented a novel wing design method for the conceptual design phase of an aircraft [2]. This method uses a robust aerodynamic database to map transonic effects and, optionally, the potential of innovative technologies. The capability of the method was demonstrated with various application cases for both turbulent and laminar aircraft. However, the method offers potential for further development. The motivation for these advancements and the derived paper objectives are outlined in the next part.

### 1.1 Motivation

In times characterized by climate, geopolitical, and energy crises alongside economic downturns, improving aircraft concerning reducing emissions, costs, and dependence on fossil energy sources is imperative [3–5]. For this, enhancing the aerodynamics of the aircraft offers great savings potential. Two promising technologies to improve aerodynamics are hybrid laminar flow control (HLFC) and variable camber (VC). The individual capabilities of HLFC and VC have been demonstrated in various publications [6–11]. However, the combined impact of these technologies on the overall aircraft design (OAD) remains an ongoing research subject. The German LuFo VI-1 project *CAT<sub>2</sub>W* (Coupled Aerodynamic Technologies for Aircraft Wings) was initiated to address this research gap. The general idea is to maximize the effect of the technology composition in synergistic action. While initial results indicate the retrofit potential for efficiently utilizing the synergy between HLFC and VC [12, 13], the integration as add-on solutions inherently limits their full potential. Initially, the novel wing design method mentioned above optionally considers laminarity as a driving design factor. Hence, the next step in developing the method is investigating whether VC can also be considered already in the wing design process. The resulting objectives of this paper and the chosen approach are explained next.

## 1.2 Paper objectives and approach

The overall objective of this paper is to further improve and extend the wing design method presented in Ref. [2]. As stated above, one of the ideas is to extend the scope of the method with the consideration of the VC technology. Other ideas involve punctual method improvements, e.g., considering structural effects. In order to follow the changes of the method, a short, not exhaustive overview of the wing design method is given in Sec. 2. In Sec. 3, the extensions and improvements of the method are explained. In Sec. 4, we present results from different application cases, highlighting the effects of both the single and the combined changes. Finally, concluding remarks and an outlook are given in Sec. 5.

## 2. Introduction to wing design method

The novel wing design method enables a detailed, transparent but still runtime-efficient design process for the in-house conceptual aircraft design environment MICADO<sup>1</sup> [2]. To follow the advancements discussed in Sec. 3, the initial status of the method is summarized first. However, only the most relevant parts of the method are outlined; for a more detailed discussion and initial application cases, the reader may refer to Refs. [2, 17]. The design process, which is depicted in Fig. 1, generally consists of two modules.

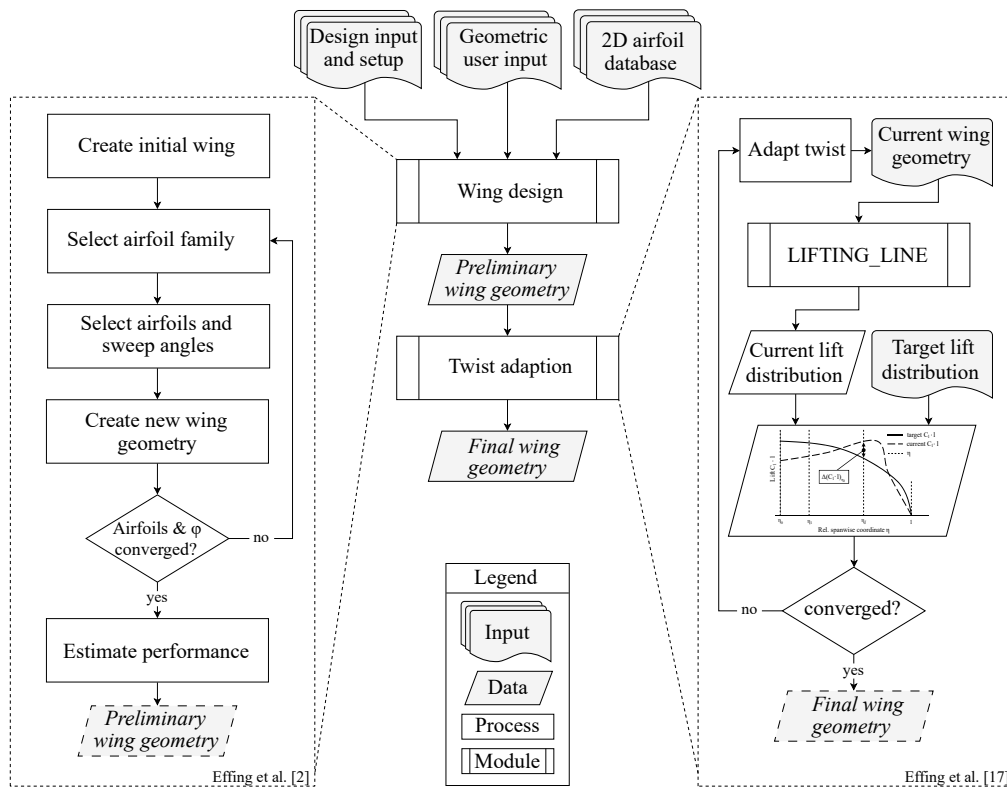


Figure 1: Process chain of the wing design methodology presented in Ref. [2]

The first module comprises the central part of the method and is also the part for which advancements are presented in this work. This wing design approach is implemented in Matlab [18] and processes the input data, automatically selects suitable airfoils from a database, and optimizes the sweep angles for user-selected performance indicators. The input consists of design data such as the top-level aircraft requirements, initial estimations of the operating empty mass (OEM) and maximum take-off mass (MTOM), and the targeted shape of the lift distribution. The distribution is then derived from the required lift of the wing, which is calculated utilizing the following assumption from Sadraey [19]:

$$C_{L,wing} = \frac{1}{0.95} \cdot C_{L,aircraft} = \frac{1}{0.95} \cdot \frac{2 \cdot m_{av} \cdot g}{\rho \cdot v_{\infty}^2 \cdot S_{ref}}. \quad (1)$$

<sup>1</sup>Multidisciplinary Integrated Conceptual Aircraft Design and Optimization environment [14, 15]; MICADO is an internal specialization of UNICADO [16] providing conceptual design methods with increased fidelity.

The reference area  $S_{\text{ref}}$ , the density  $\rho$ , and the flight speed  $v_{\infty}$  are derived from the predefined wing loading, flight altitude  $h_{\text{cr}}$ , and cruise Mach number  $\text{Ma}_{\text{cr}}$ . The average mass  $m_{\text{av}}$  is calculated using the following relation:

$$m_{\text{av}} = \frac{OEM + MTOM}{2}. \quad (2)$$

The resulting design point is used throughout the whole design process, making the wing *one-point optimized*. Required changes to this assumption to consider VC are discussed in Sec. 3.3. In addition, the input includes geometric parameters such as the taper ratios  $\lambda$  and the thickness distribution, and a SQL database. This robust database is the key element of the method and holds comprehensive 2D aerodynamic data for a catalog of airfoil families [1]. Each airfoil family consists of unique geometries that share specific characteristics but differ, e.g., in their maximum thickness. The general assumption, confirmed in internal tests [20], is that aerodynamic data within an airfoil family can be interpolated in a certain range. The database is set up using the 2D flow solver MSES [21] for numerous variations of lift coefficient, Mach number, and Reynolds number. If the user wants to consider laminarity, e.g., to design wings with integrated hybrid laminar flow control, the database is optionally set up with data for different transition positions. Automatic calculation refinement and post-processing steps, e.g., identifying the drag-divergence Mach number for every lift coefficient, provide sufficient data quality and availability in the subsequent wing design process [1].

For a swept wing, the data from the database cannot be used directly to design a 3D wing because the pressure distribution and the resulting aerodynamic forces are solely influenced by the flow perpendicular to the surface curvature [22]. However, by applying various transformation rules for the flow characteristics and the geometry, the 2D data from the database is transferred to the 3D wing object, and vice versa. On the one hand, relations originating from the simple-sweep theory are used for the freestream conditions [22, 23]. On the other hand, the geometry is transformed with the local sweep transformation accounting for varying local sweep angles of a tapered swept wing segment [23]. The primary objective of utilizing these transformation rules is to use more comprehensive data compared to traditional handbook methods while maintaining the relatively low computational demand in conceptual design phases. These methods enhance result accuracy, allow evaluating innovative technologies with no empirical data, and facilitate the development of methodologies similar to the one presented in this work. However, it should be noted that these methods do not serve as substitutes for high-fidelity computational methods. This limitation primarily arises from simplifying three-dimensional flow phenomena and the uncertainties stemming from applying the transformation rules to geometry and flow characteristics; this was already demonstrated and discussed in prior work at ILR, e.g., in Refs. [24, 25]. It is essential to clarify that the intended purpose of 2.5D methods is explicitly not to obtain final absolute values but rather to determine relative deltas between different use cases. Therefore, these methods offer remarkable advantages in evaluating the potential of new technologies; still, the next steps in the design remain high-fidelity computations and optimizations.

Following the approach of the first module on the left side in Fig. 1, an initial wing is created based on the input data. An exemplary wing resulting from this step is illustrated in Fig. 2.

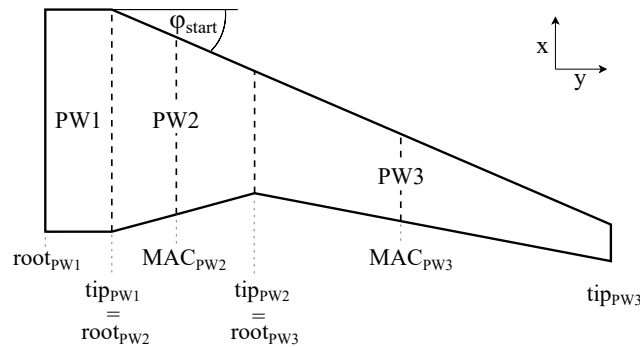


Figure 2: Exemplary initial wing geometry

Note that the initial planform results from geometric input and an initial leading edge (LE) sweep angle defined by the user and solely marks the starting point for the next design steps. Regardless of the defined start conditions, the initial wing consists of three part wings (PW) with characteristic stations (root, mean aerodynamic chord (MAC), tip). Next, a suitable airfoil family is identified for the current wing planform, and appropriate airfoil variations within the selected family and optimal sweep angles are determined. These steps involve a ranking for each station of both wetted part wings<sup>2</sup>, utilizing a multi-criteria decision-making (MCDM) process. Although the ranking method remains

<sup>2</sup>Following the Airbus definition of the reference area of the wing [26], the taper ratio and sweep angles of the fuselage segment (PW1) are always set to 1 and  $0^\circ$ , respectively.

## ADVANCEMENTS IN THE DEVELOPMENT OF A NOVEL WING DESIGN METHOD

consistent, the candidates for selection differ between the two steps: During the airfoil family selection, the candidates encompass various families within the database. The subsequent airfoil and sweep selection involves considering all airfoil variations within the chosen family and sweep angles within a specified range. Notably, while the characteristics at a specific station remain constant, the transformed data varies for each sweep angle candidate. The ranking process of both steps employs eight airfoil performance indicators, such as the lift-to-drag ratio at the required local lift coefficient  $((C_l/C_d)_{local})$  and the distance to the local drag-divergence Mach number  $(\Delta Ma_{dd})$ . All ranking parameters are slightly adapted from the ones Sadreay [19] proposes for the selection of suitable airfoils, and are acquired from the 2D database by transforming the local values of Mach number, lift coefficient, Reynolds number, and maximum airfoil thickness at each station with the current local sweep. Subsequently, a backtracking quadrilinear interpolation is used for these four dimensions to return the respective aerodynamic data from the database. The data is then used to rank the available candidates. For this, the so-called TOPSIS<sup>3</sup> method is utilized [27]. This prominent MCDM method ranks multiple alternatives by evaluating different criteria [28]. To include information about their importance, the different criteria are weighted. The corresponding weights are determined using a combinative method proposed by Jahan et al. [29]:

- Entropy method: This objective method considers the differences in the criteria between individual candidates. A criterion has less importance if all candidates perform similarly on that specific criterion. [27, 30]
- Inter-criteria correlation method: This objective method considers criteria importance through inter-criteria correlation. Hence, the data are weighted according to their correlation value with each other. This prevents criteria with the same significance from being weighted too heavily and others from being neglected. [31]
- Direct weighting method: In this method, subjective weighting, specified by the user, is applied. Here, active intervention can adjust the weighting in the desired direction. By default, the subjective individual weightings are always equally distributed.

These weighting methods are used combinatorially in the ranking process to weight the data of the individual performance indicators. The advantage of this combination is that the total weighting is not based only on a single subjective or objective weighting [29]. The total weighting of a criterion  $i$  is calculated as follows:

$$W_{total,i} = \frac{\sqrt[3]{W_{entr,i} \cdot W_{corr,i} \cdot W_{subj,i}}}{\sum_i \sqrt[3]{W_{entr,i} \cdot W_{corr,i} \cdot W_{subj,i}}} \quad (3)$$

Based on the total weighting of the single parameters, the TOPSIS method can be employed to rank all candidates. The resulting ranking points (RP) are scaled within a  $0 \leq RP \leq 1$  range, with 1 indicating the highest value. A comprehensive ranking of all available candidates is derived by combining the rankings obtained from all three stations of a part wing. Subsequently, the average of the ranking points for the part wings is computed, yielding a final ranking for the given conditions. It is important to note that as the design process progresses, the wing's geometry and aerodynamic properties may change, necessitating the repetition of the selection process in each iteration step. As a result, determining the optimal airfoil family, followed by selecting appropriate airfoil variations and sweep angles, is performed iteratively to ensure an accurate match for the evolving requirements. The starting point of each iteration is the wing geometry newly created with the identified airfoils and sweep angles.

After convergence, the performance of the resulting wing is estimated using the specific air range of the wing

$$SAR_{wing} = \frac{a \cdot Ma_{cr} \cdot L/D}{m_{wing} \cdot g} \quad (4)$$

with the local speed of sound  $a$ . The  $SAR_{wing}$  can already be determined as it is—in contrast to the conventional definition of the SAR—independent of other component masses and the engine performance. For the lift-to-drag ratio  $L/D$ , the design lift coefficient (Eq. (1)) and the profile drag composed of viscous and wave drag are used. The wing mass  $m_{wing}$  is obtained by using a semi-empirical relation proposed by Ref. [32]:

$$m_{wing} = 2.20013 \cdot 10^{-4} \cdot (401.146 \cdot S_{ref}^{1.31} + MTOM^{1.1038}) \cdot (t/c)_{rep}^{-0.5} \cdot \Lambda^{1.5} \cdot \frac{1}{\cos(\varphi_{25})}, \quad (5)$$

$$\text{with the representative thickness } (t/c)_{rep} = 0.6 \cdot (t/c)_{root,PW2} + 0.3 \cdot (t/c)_{tip,PW2} + 0.1 \cdot (t/c)_{tip,PW3}. \quad (6)$$

Notably, in the status presented in Ref. [2], the wing mass was calculated using only the quarter-chord sweep angle of the inboard part wing. This assumption leads to constant mass values between two wing geometries if—with otherwise

<sup>3</sup>Technique for Order Preference by Similarity to Ideal Solution

constant design data—the inboard sweep is equal. Hence, the outboard sweep has no influence on the mass estimation. However, the wing mass was solely used for performance estimation. Considering an initial coupling of aerodynamics and structures using this mass component is part of aspired method advancements and is discussed in Sec. 3.1. This step concludes the first module and, thus, the design of the preliminary wing geometry.

In the second module from Fig. 1, the shape of the lift distribution is tailored towards the target distribution using DLR’s multi-lifting-line code LIFTING\_LINE [33, 34]. This is achieved by automatically adapting the twist angles of each station along the wingspan; it ensures that the input lift distribution, used to select the airfoils and sweep angles, is actually achieved in the subsequent overall aircraft design loop.

To summarize, the novel wing design method starts from the airfoil level and designs a one-point optimized clean wing for the available data. Using minimum user input, predefined airfoil performance indicators, and an aerodynamic 2D database, the method automatically selects an airfoil family and, subsequently, the most suitable airfoil-sweep combination for every part wing. The approach is implemented in Matlab and converges in less than a minute runtime. Therefore, it has capabilities for clean sheet designs and mapping complex flow phenomena while keeping computational effort low. Additionally, it allows considering new technologies in an early design stage; in Ref. [2], this was demonstrated exemplary for hybrid laminar flow control. In the next section, further developments of the first module in Fig. 1, especially to consider the VC technology, are presented.

### 3. New developments in wing design method

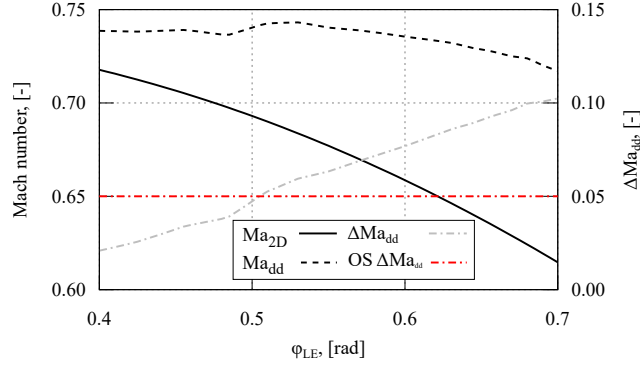
This section presents the latest advancements of the first module of the wing design (left side in Fig. 1). In Sec. 3.1, an initial coupling of aerodynamics and structures is presented. Then, a new handling of the  $\Delta Ma_{dd}$  criterion is explained in Sec. 3.2. Finally, the consideration of VC is discussed in terms of required pre-studies and method changes (Sec. 3.3).

#### 3.1 Consideration of mass

The first change to the design method is how the influence on the wing mass is considered. Before, merely the inboard sweep angle influenced the calculated mass, which, moreover, was only used for performance estimation of the resulting wing geometry (see Sec. 2). Hence, the design focused completely on aerodynamic effects. The first change foresees an average sweep angle of the wetted part wings for calculating the wing mass with Eq. (5). Now, detrimental mass effects of changes in the outboard sweep angle are no longer neglected for calculating the  $SAR_{wing}$ . Another more significant change is that a specific wing mass factor ( $f_{mass}$ ) is used as an additional ranking parameter on top of the other eight performance indicators (see Sec. 2). This factor is derived for every sweep candidate and considers both the  $1/\cos(\varphi_{25})$  relation from Eq. (5) and an assessment of how significant a change in wing mass is compared to the MTOM. Utilizing this mass factor in the ranking approach is the first step towards coupling aerodynamic benefits and adverse mass effects due to increasing sweep angles. In order to create an equivalence between aerodynamics and structures, the subjective weighting method is adapted. Before, subjective weighting was only used to provide an option for influencing the ranking, e.g., to prefer one ranking criterion over another. Now, the subjective weights are equally split up between aerodynamics and structures. This differentiation intends preventing the other eight aerodynamic criteria from overshadowing the single structural ranking criterion. Currently, only the new criterion is a structural one and is therefore weighted subjectively with 50 %; this can be adapted in further developments if more structural aspects may be considered in the design. However, this seemingly high subjective weight of 50 % is not directly transferred to the TOPSIS process since it is only one of three influencing factors for the total weight in Eq. (3).

#### 3.2 Handling of $\Delta Ma_{dd}$ criterion

The adaption of the handling of the  $\Delta Ma_{dd}$  criterion intends to avoid a too strong influence of increasing  $\Delta Ma_{dd}$  values. The reason for this change is illustrated in Fig. 3, which shows the course of the transformed Mach numbers (solid line) and the drag-divergence Mach numbers (dashed line) for an exemplary station of the inboard part wing with increasing sweep angle. Additionally, the resulting  $\Delta Ma_{dd}$  values are plotted in grey. Note that the  $Ma_{dd}$  values vary with sweep as transformation results in different Reynolds numbers and lift coefficients for every sweep candidate. Before the adaption, a candidate was considered better, the larger the offset between the cruise Mach number and the drag-divergence Mach number. Hence, in this example, the more sweep applied, the better the  $\Delta Ma_{dd}$  criterion performed. However, limiting the beneficial effect once a user-defined offset (OS) is reached seems more reasonable. For such an offset, Torenbeek [35] suggest a range of  $0 \leq \Delta Ma_{dd} \leq 0.05$ . In Fig. 3, an exemplary OS of 0.05 is indicated in red. The new handling sets all candidates surpassing this line to the offset’s value. Therefore, in this example, the  $\Delta Ma_{dd}$  values for  $\varphi_{LE} \geq 0.5$  rad are set to 0.05 resulting in no further preference with increasing sweep.

Figure 3: Exemplary analysis of  $\Delta Ma_{dd}$  criterion, adapted from Ref. [2]

### 3.3 Consideration of variable camber

One remarkable advantage of the novel wing design method is to use comprehensive aerodynamic airfoil information to map transonic effects and, optionally, the potential of new technologies. In Ref. [2], we demonstrated this for integrating HLFC. As stated in Sec. 1, another promising technology is VC. In order to include VC as another driving design factor, changes to the database setup (Sec. 3.3.1) and to the method (Sec. 3.3.2) are discussed next.

#### 3.3.1 Preliminary studies on airfoil level

For considering the VC technology already in the wing design, the 2D airfoil database must hold aerodynamic data of clean airfoils and airfoils with different flap deflections. The required airfoil geometries are illustrated in Fig. 4 in which an airfoil family consisting of airfoils with varying maximum thicknesses (left side) is extended by one dimension for ADHF<sup>4</sup> airfoil deflections (right side).

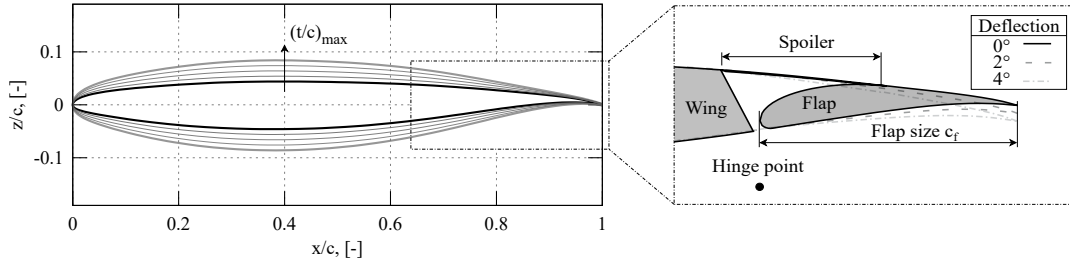


Figure 4: Exemplary dataset for an airfoil family with VC deflections

For the creation of ADHF airfoils, an internal tool is available, which requires the coordinates of the hinge point and the relative flap size  $c_f$  as input. To ensure that the wing design process is not limited to a constant flap layout, airfoils with different flap sizes must be stored in the database. In order to keep the size as well as preparation time of the database within an acceptable range for the conceptual design phase, simplifications must be made. Although the hinge point of an ADHF airfoil is usually chosen as a compromise between good Fowler movement and acceptable small unslotted deflections [37], the aim of the method is explicitly not to optimize the movement and layout of the flaps. Hence, the required dimensions of the database are reduced by using the following relations for the coordinates of the hinge point:

$$(x/c)_{hinge} = 1 - c_f, \quad (7)$$

$$(z/c)_{hinge} = -0.3 c_f - 0.01. \quad (8)$$

Hence, the  $x$  coordinate of the hinge point is fixed at the flap's leading edge. The  $z$  position is assumed to be below the flap and changes with the flap size. These relations are based on hinge point positions from prior VC retrofit designs at ILR, e.g., in Ref. [12], and were then derived in internal studies considering both aerodynamic benefits and detrimental effects of the positioning [38]. In the design process, the aerodynamic data of the flap sizes are interpolated to avoid storing airfoils in the database for every possible flap layout. Hence, to minimize the computational effort in

<sup>4</sup>The Adaptive Dropped Hinge Flap (ADHF) concept was selected as the VC concept with the highest weighted sum model score in the scope of the CATeW project [36]. Note that the extension of the method is not ADHF exclusive; other VC concepts can also be considered as long as the creation of the VC airfoils is adapted accordingly.

creating the database, the number of airfoils with different flap sizes should be as small as possible. Since this implies interpolations between different flap sizes, preliminary studies on airfoil level using MSES are conducted to identify sufficient database density. As an initial assumption,  $\Delta c_f = 0.1$  compromises the required calculation time and aspired accuracy. For the analysis of the interpolation error, drag polars from airfoils with two different flap sizes ( $c_f = 0.2$  and  $c_f = 0.3$ ) are interpolated to a target flap size ( $c_f = 0.25$ ). Additionally, a drag polar for an airfoil with the target flap size is calculated directly and then compared with the interpolated polar. The parameter variations for the studies reflect cruise flight characteristics and include different ADHF flap settings, airfoil thicknesses, and freestream conditions via Reynolds and Mach numbers; all parameter combinations can be found in the lower box in Fig. 5b. In Fig. 5a, an exemplary result of the pre-studies is shown. The interpolated and directly calculated drag polars are plotted in black. For a better overview, the relative interpolation error is shown in grey.

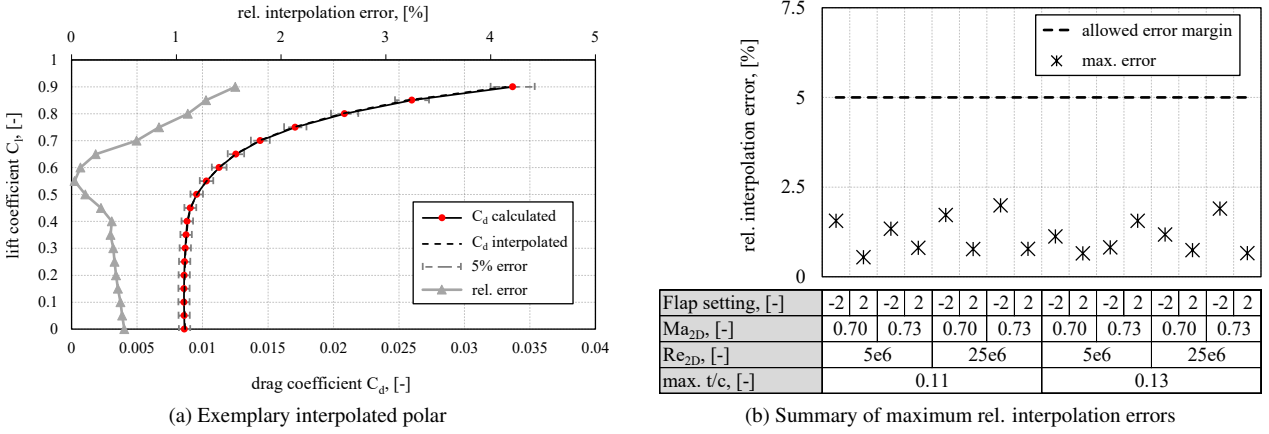


Figure 5: Results from pre-studies to ensure sufficient interpolation accuracy

It shows that the relative interpolation error stays well below the marked error range of 5%, with a maximum error of about 1.5%. This interpolation quality holds for all investigated cases, as the maximum interpolation errors of all studies are below 2% (see upper part of Fig. 5b). Based on these findings, the step width of the relative flap sizes for the database is set to  $\Delta c_f = 0.1$ . If even more accurate results are desired, this step width can be decreased. Next, the changes in the design method are presented.

### 3.3.2 Changes in design method

The adapted approach involves an advanced strategy that encompasses the selection of airfoil family, specific airfoils, and sweep angles not solely predicated upon the design characteristics of a clean wing but also takes into account the performance under off-design conditions, wherein flaps are used. This approach reflects the potential of VC technology, as it can mitigate the performance shortfall during off-design conditions by adjusting the airfoil geometry throughout the mission. In Fig. 6, the required changes to the existing method are highlighted in red. Consequently, the changes take place exclusively in the first module from Fig. 1. Besides the changes in the setup of the database discussed in Sec. 3.3.1, the main changes include the definition of off-design conditions and a flap layout by the user and an additional ranking for the off-design case reflecting the potential increase in off-design performance due to the available flap permutations. The individual points are discussed next.

**Determination of off-design conditions** During steady cruise flight, aircraft mass and, thus, lift coefficients change constantly. Consequently, the wing is no longer in the aerodynamic optimum, represented by the global design lift coefficient from Eq. (1). To account for a change in the lift, VC aims to shift the aerodynamic optimum toward the deviating coefficients in the off-design ( $C_{L,OD}$ ). For this reason, a shifted  $C_{L,OD}$  is determined first; the additional consideration of a second operating point results in a wing optimized for two points. To determine  $C_{L,OD}$  and its distribution along the wingspan, a user-defined deviation  $\beta$  of the average cruise mass from Eq. (2) is used:

$$m_{OD} = (1 - \beta) \cdot m_{av} = (1 - \beta) \cdot \frac{OEM + MTOM}{2}. \quad (9)$$

The deviation factor  $\beta$  can be either positive or negative, depending on the desired off-design conditions for which the user wants to design the wing.

## ADVANCEMENTS IN THE DEVELOPMENT OF A NOVEL WING DESIGN METHOD

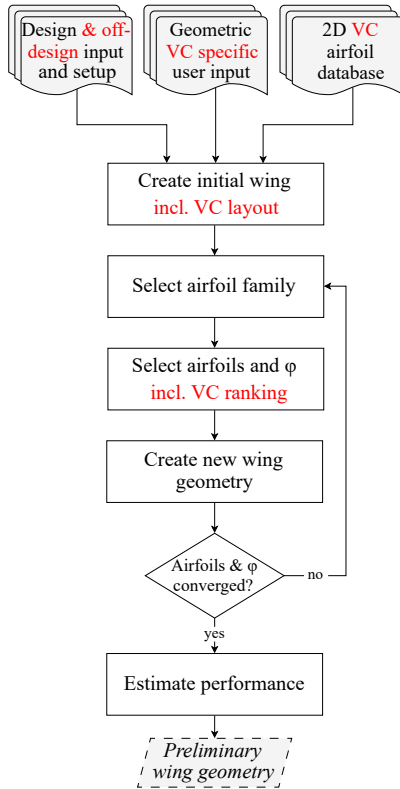


Figure 6: Approach to consider VC in wing design method

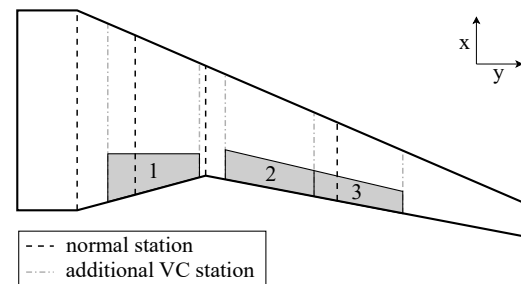


Figure 7: Exemplary initial wing geometry with VC layout and additional stations

**Definition of VC layout and creation of initial wing** In order to allow the adaptation of the wing geometry to the different operating points, the layout of the ADHF system has to be specified. Since the wing design does not explicitly lay out the control surfaces, the user specifies key points, such as the flaps' number, positioning, and geometry. Based on this, new stations are automatically inserted. Consequently, when the optional VC wing design is activated, not only three stations per part wing (see Fig. 2) but, according to the number of flaps, more stations are used for the selection process. An exemplary starting wing geometry with three flaps and the respective additional stations is illustrated in Fig. 7. The additional stations are used together with the default stations for all following steps of the method. The general segmentation into three part wings, however, is not changed.

**Off-design ranking** The candidates for the selection process are no longer ranked solely based on a single design point. Instead, an additional off-design ranking is conducted. In the design ranking, aerodynamic data is interpolated from the transformed local values of Mach number, lift coefficient, Reynolds number, and airfoil thickness. For the off-design ranking, the chosen VC layout adds the flap size as an additional dimension. Therefore, a backtracking quintilinear interpolation is used for these five dimensions to return the respective aerodynamic data from the database. Another fundamental change in the ranking approach is—apart from assessing all possible combinations of the individual flaps of a part wing—including an angle of attack distribution along the span. Before, the 3D wing and the 2D airfoils were connected through transformed local lift coefficients, thereby neglecting the corresponding angles of attack  $\alpha$ . This handling has been permissible since the subsequent twist adjustment ensures that the specified load distribution is achieved at the design point (see right side of Fig. 1). In the design process with additional consideration of VC, however, the aerodynamic data of the deployed airfoils for the off-design ranking needs to be queried for a valid interval of  $\alpha$  values to simulate a geometrically consistent wing. This interval comprises the previously identified local angles of attack of the design point and discrete  $\Delta\alpha$  values simulating a global wing pitch. Since the latter affects the whole wing equally, the values are prescribed as 3D and consequently transformed to 2D with  $\alpha_{2D} = \alpha_{3D}/\cos(\varphi_{ref})$ , thereby using simple-sweep theory by Busemann [22]. This process is depicted in Fig. 8a. It shows that for each valid airfoil-sweep combination at each station, the local angle of attack is used to identify a range of suitable options for the off-design assessment. Due to variations in angles of attack and their corresponding lift coefficients, the target load distribution is either not fully or only partially achieved during off-design conditions. Nonetheless, this

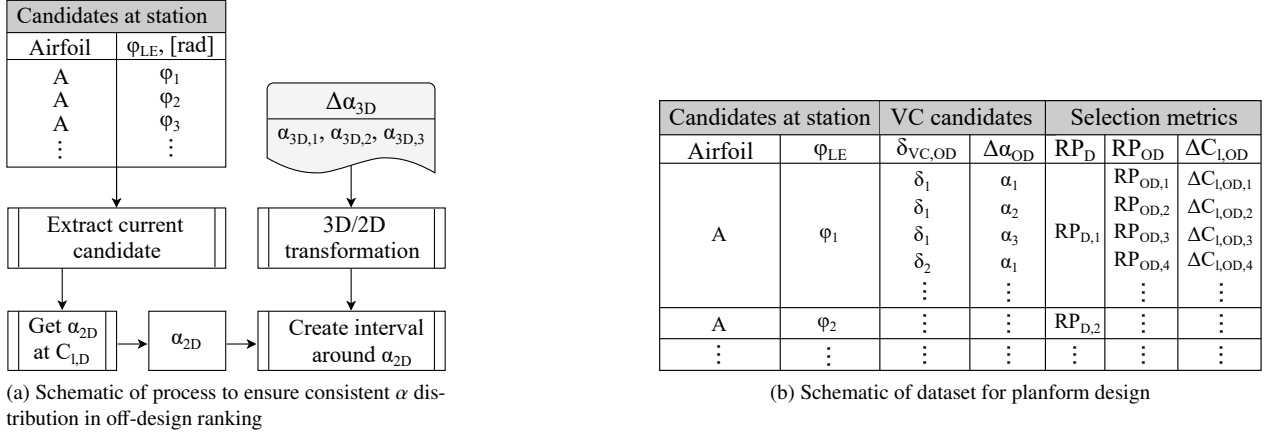


Figure 8: Schematics for the selection process considering VC deflections and pitch in off-design conditions

discrepancy, represented by the deviation  $\Delta C_{l,OD}$ , is considered in the selection process. For each VC permutation of each airfoil-sweep candidate, the performance indicators from the database are then processed in a separate TOPSIS ranking, resulting in new off-design ranking points  $RP_{OD}$ . Analogously to the previous approach, a ranking is also conducted for every airfoil-sweep candidate at the design point; this results in design ranking points  $RP_D$ . Note that the design ranking point of each airfoil-sweep candidate is assigned to its subset of VC candidates. The resulting dataset is shown in Fig. 8b. Finally, this data are used for the airfoil and sweep selection explained next.

**Airfoil and sweep selection** The last change affects the selection of airfoils and sweep angles, in which no longer only the ranking of the design point is considered. Instead, the whole dataset from Fig. 8b is taken into account. Beforehand, however, it is checked that all VC candidates are valid for all stations of the corresponding flap; disregarding invalid candidates ensures that only consistent and valid flap settings are considered further. While the ranking points should be as high as possible, the opposite holds for  $\Delta C_{l,OD}$ . The selection starts with identifying the most suitable  $\delta_{VC,OD}-\Delta\alpha_{OD}$  pairs per sweep candidate and station in off-design conditions. This pre-selection is done using the following equation:

$$\Psi_{comb} = W_D \cdot RP_D^* + W_{OD} \cdot (0.5 \cdot RP_{OD}^* + 0.5 \cdot \Delta C_l^*), \quad (10)$$

where \*-values represent the normalized distances to the corresponding optima with the off-design parameters being weighted equally. The subjective weights  $W$  allow prioritizing either the design case or the off-design case; the weights are equal by default. If only one airfoil variation is available,  $RP_D^*$  is 0 (see Fig. 8b). Since the distances should be minimized, the smallest  $\Psi_{comb}$  represents the optimum candidate. This pre-selection is done for every station of a part wing and yields the most suitable off-design settings for every sweep candidate. Next, the ranking points ( $RP_D$  and  $RP_{OD}$ ) of all stations of a part wing are combined; additionally, the deviation  $\zeta$  from the target  $C_{l,OD}$  distribution is approximated using the  $\Delta C_{l,OD}$  values of all stations. This approach yields three metrics per sweep candidate of the whole part wing and allows the final selection according to the following equation:

$$\Psi_{comb,PW} = W_D \cdot RP_{D,PW}^* + W_{OD} \cdot (0.5 \cdot RP_{OD,PW}^* + 0.5 \cdot \zeta^*). \quad (11)$$

Once the optimal sweep angle is identified, the most suitable airfoils with their off-design flap positions and associated pitch angles are selected. The final off-design data are only used for subsequent analyses of the results. They are not further considered in the aerodynamic analysis in the overall aircraft design loop. For more information about the approach to analyzing aircraft with coupled HLFC and VC technologies in MICADO, the interested reader is referred to Effing et al. [12]. The convergence of the adjusted process in Fig. 6 results in a wing geometry that is *two-point optimized*, assuming that VC flaps can boost the performance in off-design conditions.

## 4. Application

In this section, various application cases are presented. In order to highlight the influence of the single changes described in Sec. 3, the studies are structured as follows: In Sec. 4.1, the input data and the resulting reference configurations are briefly introduced. Using these references, punctual analyses of the influence of the changes from Secs. 3.1 and 3.2 are presented in Sec. 4.2. The section concludes with analyses of the influence of the consideration of VC and, thus, a two-point optimization (Sec. 4.3).

#### 4.1 Input data and reference configurations

The following application studies utilize a database with airfoils adapted from the AVACON project [39] and representing one airfoil family. Limiting the number of airfoil families helps in focusing on the effects of the method advancements. Hence, the airfoil family selection (see Fig. 1) is obsolete for the following applications. In addition to the clean airfoils shown in the left part of Fig. 4, data for various ADHF permutations are available in the database. The resulting database comprises permutations with flap sizes  $c_f = 0.2$  and  $c_f = 0.3$ , all created using the hinge point definition from Eqs. (7)-(8). Note that the available flap sizes limit the possible VC layouts; however, more freedom in defining the layout can be achieved by storing more airfoil variations in the database. For these flap sizes, VC deflections range from  $-2^\circ \leq \delta_{VC} \leq 4^\circ$  with  $\Delta\delta = 1^\circ$ . All following studies are conducted for a short-range (SR) and a medium-range (MR) aircraft; the relevant input data is listed in Tab.1. Additionally, a 3D thickness distribution is manually specified (see Fig. 9).

Table 1: Input data for application cases

Parameter	Unit	Range type	
		SR	MR
$Ma_{cr}$	-	0.78	0.83
$h_{cr}$	ft	33 000	35 000
span b	m	34	52
MTOM	kg	77 000	137 000
OEM	kg	42 000	80 000
W/S	kg/m <sup>2</sup>	640	622
span fuselage segment	m	4	5.18
$\lambda_{PW}$	-	[0.55, 0.30]	
rel. kink position $\eta_{kink}$	-	0.37	0.313
$\varphi_{LE,start}$	rad	0.40	
$\varphi_{LE,max}$	rad	0.70	

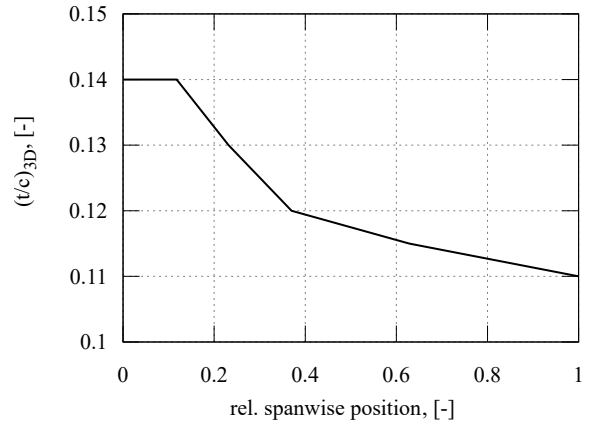


Figure 9: Predefined 3D thickness distribution

In this work, all wings are designed targeting an elliptical load distribution. Note that the status of the method and the input data of the references mirror the application cases presented in Ref. [2]. Therefore, the designed reference wings are not explicitly analyzed. Compared to the designs from Ref. [2], slight sweep angle changes result from focusing on one airfoil family and minor improvements in the setup of the 2D airfoil database and the associated available aerodynamic data. Figure 10 shows the planform views of the reference configurations.

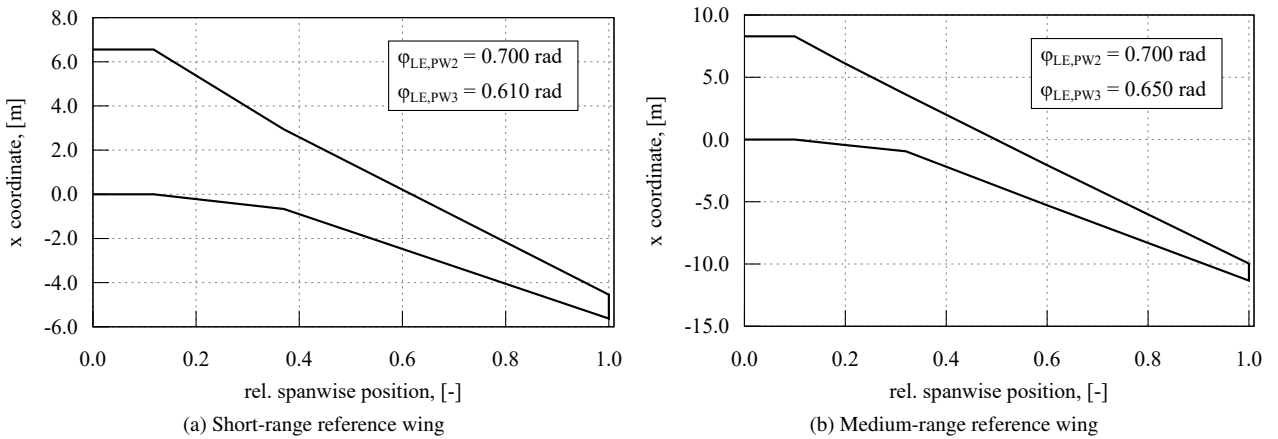


Figure 10: Reference wing geometries

The maximum allowed sweep angle of  $\varphi_{LE} = 0.7$  rad is selected for both inboard part wings. Hence, this sweep angle is the best candidate for the given set of objectives, as most ranking criteria favor high sweep angles for the local design conditions. The outboard part wings, however, differ, with a higher sweep angle for the MR reference. This difference is mainly due to the increased Mach number and its influence on the aerodynamic data of the individual stations; for a deeper analysis of the underlying ranking process, the reader is referred to Ref. [2].

## 4.2 Influence of the changes on wings without VC consideration

This section presents the influence of the changes described in Secs. 3.1 and 3.2. The changes are considered step-by-step, with all changes active for the final design case. Note that since the database used for the studies holds data only for one family and one clean airfoil variation, the changes influence only the selection of the sweep angles.

### 4.2.1 Short-range application studies

Starting with the short-range input data from Tab. 1, the resulting leading edge sweep angles of all different studies are summarized in Fig.11; for a better overview, the sweep angles of the SR reference wing are marked on the right side. In the following, this bar chart is used for punctual analyses.

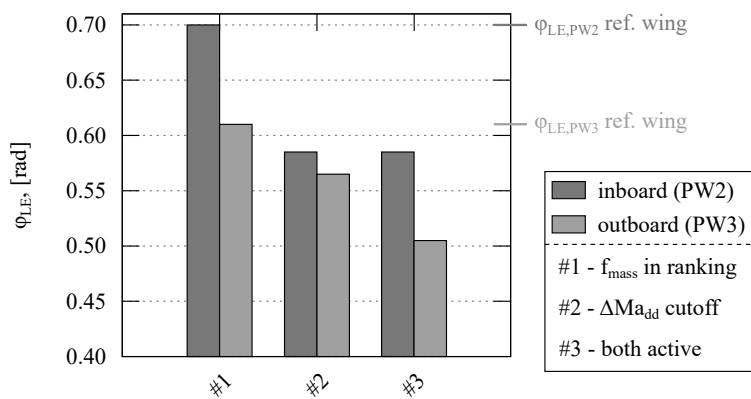


Figure 11: Summary of studies for short-range reference

**Study #1 ( $f_{mass}$  in ranking)** Comparing the data with the leading edge sweep angles of the SR reference wing reveals no influence of the additional consideration of the wing mass (#1), although the mass criterion is already weighted subjectively with 50 %. However, the subjective weight is not directly used in the ranking, as it is combined with the weights of the correlation and entropy methods beforehand (see Sec. 3.1). Table 2 lists the final weighting parameters for selected ranking criteria exemplary for the MAC station of the inboard part wing (PW2).

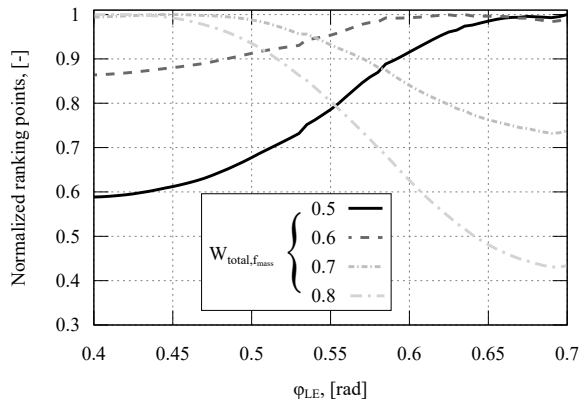
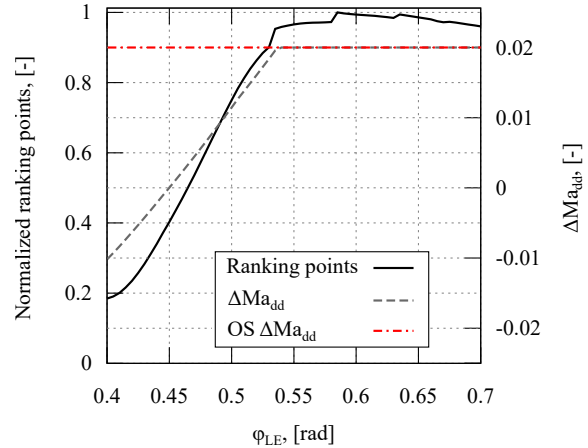
Table 2: Final weighting parameters of MAC station (PW2) for sweep selection in study #1

Weights	Ranking parameter			
	$(\bar{C}_l/\bar{C}_d)_{max}$	...	$\Delta Ma_{dd}$	$f_{mass}$
$W_{entr}$	0.1359	...	0.1093	0.1078
$W_{corr}$	0.0861	...	0.0908	0.1544
$W_{subj}$	0.0625	...	0.0625	0.5
$W_{total}$	0.0980	...	0.0928	0.2205

The data show that combining all weights results in a total weight of the mass criterion of 0.2205. This weighting is too low to influence the final selection, which is still dominated by the other aerodynamic criteria. Without any other changes, an immensely high total weighting is required for the mass factor to have an influence. Figure 12 illustrates the evolution of the normalized ranking points of the inboard MAC station for manipulated total weights of the mass factor over the range of the sweep candidates; the weights of the other parameters are distributed equally in this case.<sup>5</sup>

<sup>5</sup>Note that the trend towards low or high sweep angles results from the specific local conditions at PW2. The ranking points do not consistently exhibit such a smooth trend, as varying conditions introduce additional trade-offs among the different criteria, influencing the final ranking outcome.

## ADVANCEMENTS IN THE DEVELOPMENT OF A NOVEL WING DESIGN METHOD

Figure 12: Influence of weights of  $f_{\text{mass}}$  (MAC PW2)Figure 13: Influence of  $\Delta Ma_{dd}$  cutoff (MAC PW2)

The course of the ranking points shows that with increasing total weights, the trend towards high sweep angles first decreases before it flips at  $W_{\text{total}, f_{\text{mass}}} = 0.7$ . Hence, high total weights are required to prioritize structural aspects over the other aerodynamic criteria. This shows the very basic character of the mass consideration. However, this can be improved by a more sophisticated aero-structure coupling in the future. The new differentiation between aerodynamic and structural subjective weighting and the TOPSIS approach in general allow future adaption for adequate consideration of mass relevant criteria. In addition, these findings do not imply the new criterion having no effect on the final sweep selection; this will briefly discussed in the analysis of study #3.

**Study #2 ( $\Delta Ma_{dd}$  cutoff)** Contrary to consideration of a mass criterion in #1, the new handling of the  $\Delta Ma_{dd}$  criterion results in considerably decreased sweep angles (see #2 in Fig. 11). The effect of the cutoff on the MAC station of the inboard part wing is illustrated in Fig. 13. It shows that the cutoff margin, which is set to  $\Delta Ma_{dd} = 0.02$  in this case (dashed red line), limits the beneficial effect of constantly increasing  $\Delta Ma_{dd}$  values (dashed grey line). This cutoff results in the curve of the normalized ranking points (solid black line) deviating from its trend. Since the cutoff also influences all other stations of the wing, this deviation results in prioritizing lower sweep angles, with  $\varphi_{LE, PW2} = 0.585$  rad and  $\varphi_{LE, PW3} = 0.565$  rad.

**Study #3 (both active)** The final study for the SR reference considers both changes from Secs. 3.1 and 3.2. The corresponding bar charts in Fig. 11 reveal synergy effects between the changes. Recall that the mass criterion (with default weighting settings) does not influence the sweep selection when activated individually. However, it can change the method's outcome when combined with the new handling of the  $\Delta Ma_{dd}$  criterion; in this case, a lower sweep angle for the outboard part wing is selected. The reason for the different selection is illustrated in Fig. 14, in which the ranking points  $RP_{PW3, \text{total}}$  of the studies #2 and #3 are plotted as a function of the different sweep candidates. The final selections, thus highest ranking points, are highlighted in red. Additionally, the differences between the ranking points of studies are plotted with a solid black line.

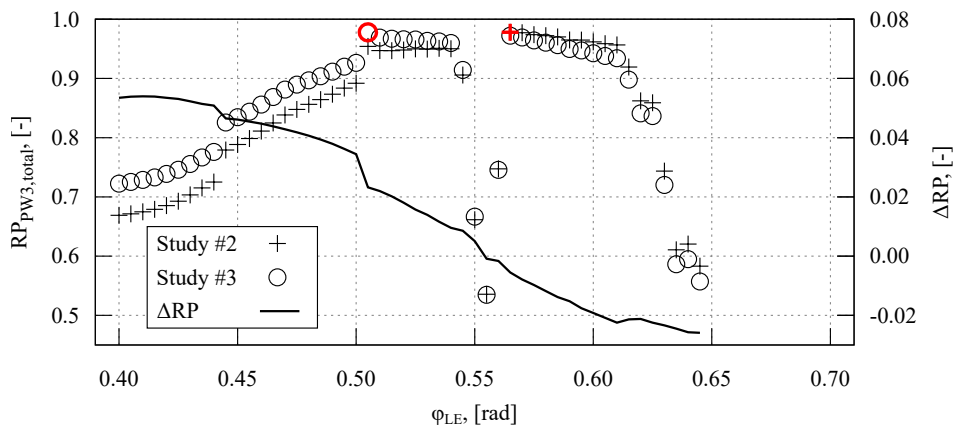


Figure 14: Comparison of final ranking points between studies #2 and #3 for the outboard part wing (PW3)

Note that the steep drop at  $\varphi_{LE} \approx 0.55$  rad originates from discrepancies in the  $Ma_{dd}$  data; however, these drops only

occur sporadically and are part of current research for the database setup. More importantly, the drops do not blur the effects of the additional consideration of the wing mass. The variations in ranking points exhibit a similar pattern to the cases where the selection process in Fig. 12 is affected by the inclusion of the  $f_{\text{mass}}$  criterion. Although the final choice in both studies is relatively close, the additional consideration of the wing mass leads to a smaller sweep angle of the outboard part wing ( $\varphi_{\text{LE,PW3,\#2}} = 0.505$  rad vs.  $\varphi_{\text{LE,PW3,\#3}} = 0.565$  rad).

The different studies outlined the potential influence of the changes to the method. Whether or not these are universal effects is discussed next.

#### 4.2.2 Medium-range application studies

For this discussion, the same three studies are conducted; however, this time, the input for the medium-range reference is used (see Tab. 1). Figure 15 shows the results of all studies; again, the sweep angles of the respective reference wing (Fig. 10b) are marked on the right side.

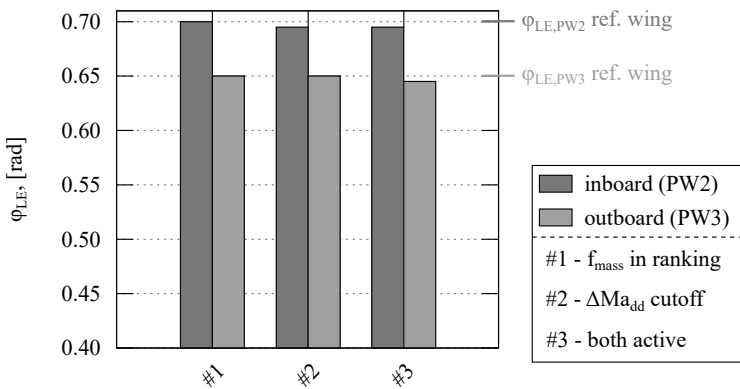


Figure 15: Summary of studies for medium-range reference

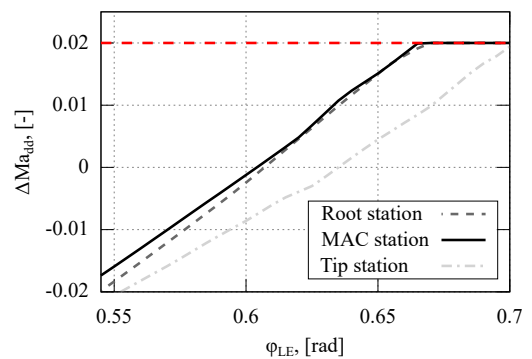


Figure 16: Influence of  $\Delta Ma_{\text{dd}}$  cutoff (PW2)

Like in the short-range application, the additional consideration of the wing mass in the ranking shows no influence on the sweep selection. This is again due to aerodynamic criteria dominating the ranking process. Contrary to the findings in Sec. 4.2.1, however, the new handling of the  $\Delta Ma_{\text{dd}}$  criterion does not influence the sweep selection significantly, with only the inboard sweep being slightly decreased to  $\varphi_{\text{LE,PW2,\#2}} = 0.695$  rad. Figure 16 illustrates the effect of the cutoff on the course of the  $\Delta Ma_{\text{dd}}$  criterion for all stations of the inboard part wing as a function of sweep candidates. As indicated by the x-axis, the minimum available sweep angle candidate is  $\varphi_{\text{LE}} = 0.545$  rad. In the case of lower sweep angles, the transformation yields 2D freestream conditions where the data of the available airfoils fail to meet the required  $C_{l,\text{max}}$  values of the user-defined lift distribution. For the remaining sweep candidates, the new handling intervenes only at the last candidates of the root and the MAC stations; the tip station is not influenced at all. Since the rankings of all stations are combined, the influence of the new handling on the final sweep selection is, therefore, small. The effect on the outboard wing is negligible, resulting in no influence of the new handling on the outboard sweep selection.

When the changes are combined in study #3, minor synergies affect the outboard wing; however, the alternative studies with different input data show that the changes to the method presented in Secs. 3.1 and 3.2 do not always influence the final wing designs considerably. This is because a) the adverse structural effects of increasing sweep angles are mostly being dominated by other aerodynamic criteria, and b) the new handling of the  $\Delta Ma_{\text{dd}}$  criterion depends on the input conditions and the subsequently queried data from the database. However, the presented changes help in classifying the influence of the  $\Delta Ma_{\text{dd}}$  criterion if more airfoil families/variations are available in the database and allow considering structural aspects, thus, another essential discipline in aircraft design; the fidelity and extent of the consideration of structural effects can be increased in future work.

#### 4.3 Consideration of variable camber

In this section, the application cases for the additional consideration of variable camber capabilities are presented; all method changes from the previous section are additionally activated. Again, the results for the short-range application cases are analyzed in detail, whereas the medium-range design briefly questions the transferability of the findings on other application cases.

### 4.3.1 Short-range application study

As described in Sec. 3.3, a VC specific layout and off-design input conditions must be defined. Table 3 lists the relevant parameters of the VC layout.

Table 3: Flap layout of short-range configuration

Parameter	inboard	outboard
relative flap size $c_f$	0.25	
$\eta_{start}$	0.18	0.37
$\eta_{end}$	0.33	0.68
flap elements	1	2

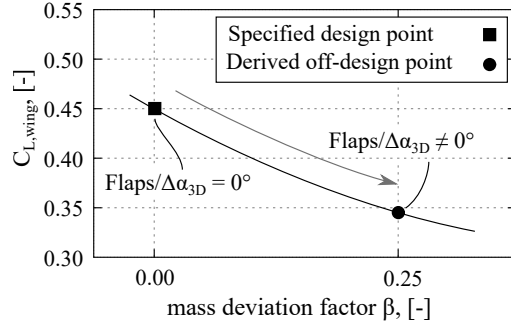


Figure 17: Off-design principle

Note that against common practice, the inboard flap is also defined with a constant relative  $c_f$ . This is due to the available database setup (see Sec. 4.1); once, a more extensive database is available, different VC layouts can be defined. For deriving the off-design conditions, an exemplary deviation factor of  $\beta = 0.25$  is used to calculate the mass (see Eq. (9)) and subsequently the lift coefficient  $C_{L,OD}$  of the wing using Eq. (1). The resulting principle for the consideration of VC is illustrated in Fig. 17. In the design conditions, both the flap deflections and the wing pitch are deactivated, while for the off-design conditions with reduced lift, both options to alter the lift distribution and, thereby, approach the scaled off-design lift distribution are activated. Although the approach for allowing flap deflections and pitch also in design conditions is generally possible with the method, it is discarded, as internal studies showed that the significantly increased runtime outweighs the benefits of more possible wing permutations [38]. Nonetheless, Fig. 18 illustrates that the approach in Fig. 17 also remarkably increases the number of possible candidates per sweep angle; recall that before, only one candidate per sweep angle and airfoil variation was considered in the selection.

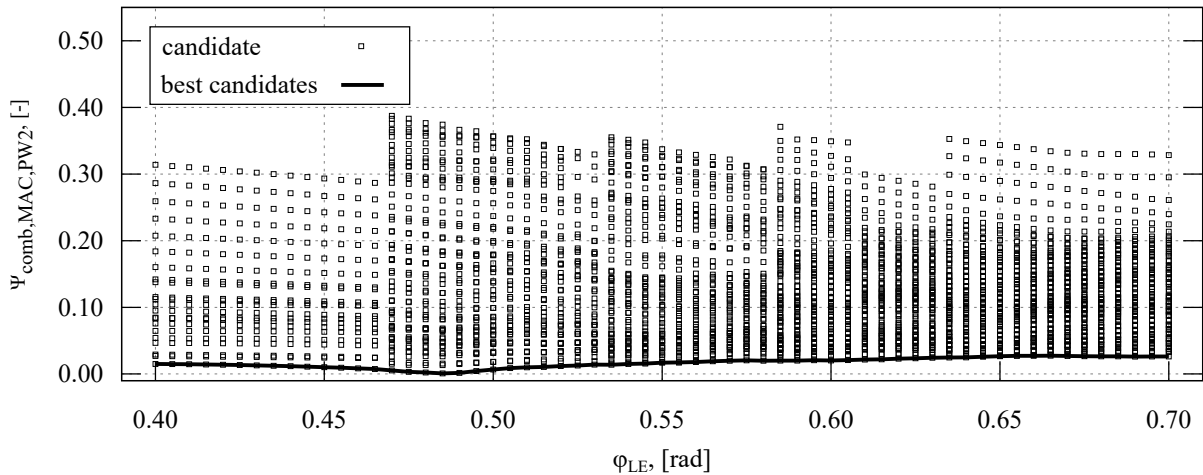


Figure 18: Pre-selection of available candidates at MAC station (PW2)

The number of candidates depends on available and valid pairs of  $\delta_{VC}$  and  $\Delta\alpha$  for each sweep angle; in this case, the total number adds up to over 3 300, all derived from Eq. (10). Note that—at this stage—the lowest  $\psi_{comb}$  values do not indicate the best candidate overall but reflect the ranking among the other possible candidates for the same sweep angle. Each sweep angle's best candidate (solid black line in Fig. 18) is subsequently combined with the ones from the other stations. After calculating the deviation  $\zeta$  of the targeted off-design lift distribution, the final ranking for the part wing is done using Eq. (11). The resulting wing and the relevant lift distributions are shown in Fig. 19; the approximated deviation area  $\zeta$ , calculated by linearly connecting the points used for the selection (blue crosses), is highlighted in grey.

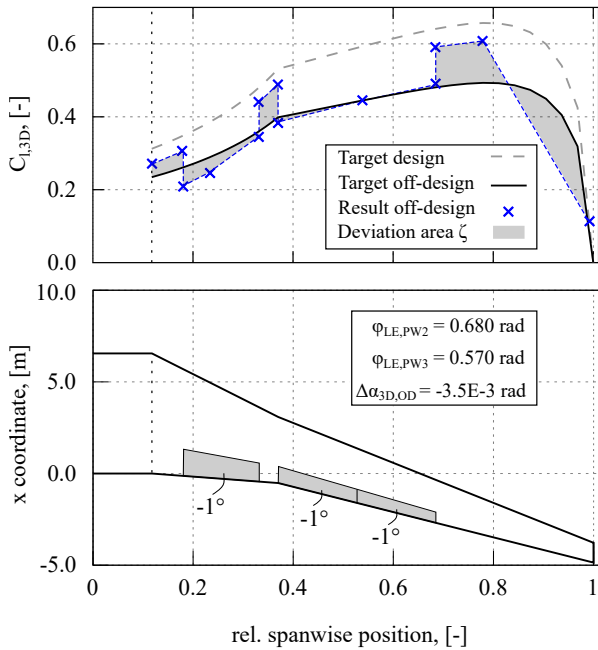


Figure 19: Results for design with VC (SR)

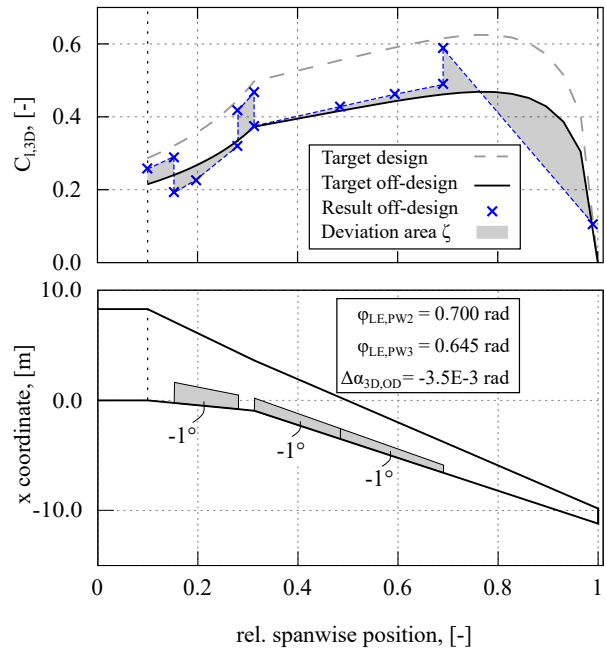


Figure 20: Results for design with VC (MR)

Recall that the result represents the most suitable sweep angles considering the (off-)design conditions and the deviation area. For the off-design, the final selection foresees a combination of flaps equally deployed by  $\delta_{VC} = -1^\circ$  and a global pitch of  $\Delta\alpha_{3D} = -3.5E-3$  rad ( $-0.2^\circ$ ). This combination approximates the target off-design lift distribution, as indicated by the blue crosses. Note that no exact match is possible due to the requirements of a geometrically consistent wing when considering both operating points (see Sec. 3.3.2). As listed in the box in the lower part of Fig. 19, the approach converges to higher sweep angles when compared to wings without the additional VC consideration (study #3 in Fig. 11). One of the reasons for this is the chosen off-design principle (see Fig. 17), as lower lift coefficients experience a trend to increasing aerodynamic performance, such as increasing  $L/D$ , with increasing sweep (and a constant Mach number). If, e.g., a mass deviation factor of  $\beta = -0.15$  is used as input, thus creating an opposite effect of the principle in Fig. 17, the sweep angles are significantly lower ( $\varphi_{LE,PW2} = 0.585$  rad and  $\varphi_{LE,PW3} = 0.52$  rad). This behavior indicates that further studies could focus on consolidating three instead of two design points ( $C_{L,OD,1} \leq C_{L,D} \leq C_{L,OD,2}$ ). However, even considering VC with only one off-design point significantly increases the computation cost, making it a special extension with up to 45 min runtime. Another approach is to include the method in the conceptual aircraft design environment MICADO for design and optimization studies. These analyses help to classify whether the special extension considerably affects the final aircraft with integrated VC technology.

#### 4.3.2 Medium-range application study

For the medium-range application case, the relative properties of the VC layout from Tab. 3 are slightly adjusted to the different kink position (see Tab. 1). Figure 20 shows the resulting planform and the relevant lift distributions. The inboard sweep ( $\varphi_{LE,PW2} = 0.7$  rad) is higher than the respective sweep of the wing without VC consideration (study #3 in Fig. 15), mirroring the effects of the short-range VC application of the previous section. However, the same sweep angle ( $\varphi_{LE,PW3} = 0.645$  rad) is selected for the outboard wing. Again, the selection results from the best compromise of the (off-)design conditions and the approximated deviation area. Therefore, the effect of the additional consideration of VC in the wing design process depends on the given input dataset and the available airfoil data. However, the upper part of Fig. 20 reveals an upcoming challenge for future developments: Currently, the deviation area  $\zeta$  is approximated by linearly connecting the points used for the selection process. Thereby, the effect of the spanwise extent of the flaps is covered, which would not be addressed if only the local  $\Delta C_{1,OD}$  values were considered in the ranking. Nonetheless, the large distance between the last two spanwise positions may distort the selection, as shifting the left point at  $\eta = 0.68$  closer to the target distribution results in a more considerable deviation of the adjacent tip segment. Although initial investigations revealed no influence on the outcome when neglecting this distorting area, better station positioning would decrease the effect. In future studies, the influence of shifting the MAC station (or adding an additional station) to already decrease the deviation area when connecting the positions used for the design point will be investigated; this may achieve a better representation of the critical aerodynamic conditions and simultaneously decreases the above-mentioned distorting effect in off-design conditions.

## 5. Conclusions and Outlook

This work presented advancements in developing a novel conceptual wing design method. The method generally foresees to design (laminar) wings using comprehensive 2D aerodynamic information stored in an airfoil database and multi-criteria decision-making processes. Based on findings from application cases with the initial method, the advancements include method improvements and extensions; all changes were first explained, and their influence subsequently demonstrated in selected application cases using a step-by-step approach. For the application cases, a database holding data of one airfoil family, clean airfoils with varying thicknesses, and respective VC permutations of the clean airfoils was utilized.

The first major change is to include basic structural effects in the selection process of airfoil-sweep combinations as an additional ranking criterion. The idea is to include detrimental effects on the mass due to the increasing sweep into the ranking process. Although subjective weighting intends to balance aerodynamic and structural criteria, the selection was still dominated by aerodynamic effects when no other method changes were considered. However, the ranking approach allows for adaption, e.g., to increase the number of mass-relevant criteria and implement more sophisticated aero-structure coupling in the future.

The second major change is a new handling of a specific ranking criterion, namely the local distance to the drag-divergence Mach number  $\Delta Ma_{dd}$ . Before, depending on the use case, constantly increasing  $\Delta Ma_{dd}$  values distorted the ranking of the candidates. Now, the beneficial effect is limited once a user-defined offset is reached. This handling prevents candidates from being ranked too heavily, even if other candidates also ensure a sufficient margin from the local  $Ma_{dd}$ . The results demonstrated a remarkable influence of the new handling, with the intended effect of high sweep angles no longer consistently dominating the ranking. Additionally, synergy effects between the two changes occur, resulting in decreased sweep angles. However, the effect strongly depends on the input data, as the influence on the outcome of the medium-range wing design was negligible.

Furthermore, an extension to the existing method was implemented to consider the variable camber (VC) technology as an additional design factor. This extension uses a database with various airfoil permutations, allowing the design of wings with different flap layouts. The required data density in the database was derived from preliminary studies on airfoil level. The new extension considers another operating point in the design process; in this off-design point, flap deflections and global pitch changes are allowed and assessed in a new, combined selection process. Compared to the wings designed for only one (design) operating point, the extension resulted mainly in higher sweep angles. This was traced back to the chosen design principle, with lower lift coefficients being used for the off-design condition; these findings hint at investigating the influence of different design principles. Since the extension significantly increases the computational costs, we intend to analyze the actual influence of considering other operating points in the wing design process on overall aircraft design level in future studies. Moreover, adjusting the currently constant positioning of the stations used for the design promises to represent the critical aerodynamic conditions better.

In addition to this punctual improvement potential, the next step is to design wings considering both laminarity and VC and to include the method in the in-house overall design environment MICADO. This step enables conclusions about the benefits of the designed wings compared to existing reference cases, such as the retrofit design with integrated hybrid laminar flow control and variable camber technologies already derived in the CATeW project.

## 6. Acknowledgments

The presented work has been carried out in the project CATeW (Coupled Aerodynamic Technologies for Aircraft Wings), funded by the German national research funding scheme LuFo VI-1 (Luftfahrtforschungsprogramm). The authors would like to acknowledge the support of the German Federal Ministry for Economic Affairs and Climate Action (BMWK).

## References

- [1] Schültke, F., Stumpf, E.: Implementation of an Airfoil Information Database for Usage in Conceptual Aircraft Wing Design Process. In: AIAA SciTech 2019 Forum. American Institute of Aeronautics and Astronautics, Reston, VA (2019)
- [2] Effing, T., Schültke, F., Heuschling, Y., Mauerer, P., Stumpf, E.: Novel Approach for Wing Design in Conceptual Overall Aircraft Design. In: AIAA SciTech 2023 Forum. American Institute of Aeronautics and Astronautics, Reston, VA (2023)

- [3] Flightpath 2050: Europe's Vision for Aviation - Maintaining Global Leadership & Serving Society's Needs: Report of the High-Level Group on Aviation Research. Policy / European Commission. Publications Office of the European Union, Luxembourg (2011)
- [4] Dreyer-Langlet, N.: Flightpath 2050-Nachfolge: Vision, Ziele, Strategien, Technologien: Impulsvortrag und Podiumsdiskussion II. In: Deutsche Gesellschaft für Luft- und Raumfahrt - Lilienthal - Oberth e.V. (ed.) 70. Deutscher Luft- und Raumfahrtkongress (2021)
- [5] European Commission: EU 'Save Energy': Communication from the Commission to the European Parliament, the Council, the European Economic and Social Committee and the Committee of the Regions, Brussels, Belgium (2022)
- [6] Joslin, R.D.: Overview of Laminar Flow Control. Tech. Rep. NASA/TP-1998-208705, NASA Langley Research Center, Hampton, VA (1998)
- [7] Braslow, A.L.: A History of Suction-Type Laminar-Flow Control with Emphasis on Flight Research, 13 edn. Monographs in Aerospace History, Washington, D.C (1999)
- [8] Schrauf, G., von Geyr, H.: Simplified Hybrid Laminar Flow Control for the A320 Fin: Aerodynamic and System design, First Results. In: AIAA SciTech 2020 Forum. American Institute of Aeronautics and Astronautics, Reston, VA (2020)
- [9] Boeing Commercial Airplane Company: Assessment of Variable Camber for Application to Transport Aircraft. Technical Report NASA-CR-158930, NASA Langley Research Center, Hampton, VA (1980)
- [10] Szodruch, J.: The Influence of Camber Variation on the Aerodynamics of Civil Transport Aircraft. In: American Institute of Aeronautics and Astronautics (ed.) AIAA 23st Aerospace Sciences Meeting (1985)
- [11] Bolokin, A., Gilyard, G.B.: Estimated Benefits of Variable-Geometry Wing Camber Control for Transport Aircraft. Technical Report NASA/TM-1999-206586, National Aeronautics and Space Administration, Hampton, VA (1999)
- [12] Effing, T., Schmitz, V., Schültke, F., Peter, F., Stumpf, E.: Combined Application of Hybrid Laminar Flow Control and Variable Camber in Preliminary Aircraft Design. In: Proceedings of the 33rd Congress of the International Council of the Aeronautical Sciences, Stockholm, Sweden (2022)
- [13] Jentys, M.M., Breitsamter, C.: Transitional Flow Modelling of a Hybrid Laminar Flow Control and Variable Camber Transonic Transport Aircraft Wing. In: Proceedings of the 33rd Congress of the International Council of the Aeronautical Sciences, Stockholm, Sweden (2022)
- [14] Risse, K., Anton, E., Lammering, T., Franz, K., Hörnschemeyer, R.: An Integrated Environment for Preliminary Aircraft Design and Optimization. In: American Institute of Aeronautics and Astronautics (ed.) 53rd AIAA/ASME/ASCE/AHS/ASC Structures, Structural Dynamics and Materials Conference: SciTech 2012, vol. AIAA 2012-1675 (2012)
- [15] Schültke, F., Aigner, B., Effing, T., Strathoff, P., Stumpf, E.: MICADO: Overview of Recent Developments within the Conceptual Aircraft Design and Optimization Environment. In: Deutsche Gesellschaft für Luft- und Raumfahrt - Lilienthal - Oberth e.V. (ed.) 69. Deutscher Luft- und Raumfahrtkongress (2020)
- [16] Schültke, F., Stumpf, E.: UNICADO - Development and Establishment of a University Conceptual Aircraft Design Environment. In: Deutsche Gesellschaft für Luft- und Raumfahrt - Lilienthal - Oberth e.V. (ed.) 69. Deutscher Luft- und Raumfahrtkongress (2020)
- [17] Effing, T., Peter, F., Stumpf, E., Hornung, M.: Approach for the Aerodynamic Optimization of the Twist Distribution of Arbitrary Wing Geometries on Conceptual Aircraft Design Level. In: Deutsche Gesellschaft für Luft- und Raumfahrt - Lilienthal - Oberth e.V. (ed.) 70. Deutscher Luft- und Raumfahrtkongress (2021)
- [18] The MathWorks Inc.: MATLAB Version 9.12.0 (R2022a), Natick, MA (2022)
- [19] Sadraey, M.H.: Aircraft Design: A Systems Engineering Approach. Aerospace series. Wiley, Hoboken, NJ (2012)
- [20] Geuking, M.: Entwicklung einer Methodik für den Aufbau von Profildatenbanken zur turbulenten Flügelauflösung. Bachelor thesis, RWTH Aachen University, Aachen, Germany (2018)

## ADVANCEMENTS IN THE DEVELOPMENT OF A NOVEL WING DESIGN METHOD

- [21] Drela, M.: A User's Guide to MSES 3.05. Tech. rep. [user guide], Massachusetts Institute of Technology (MIT), Cambridge, MA (2007)
- [22] Busemann, A.: Aerodynamischer Auftrieb bei Überschallgeschwindigkeit. In: Accademia dei Lincei (ed.) 5th Volta Conference, pp. 210–220 (1935)
- [23] Wild, J.: High-Lift Aerodynamics. Taylor & Francis Group, Milton (2022)
- [24] Schültke, F., Stumpf, E.: Cross-flow effects regarding laminar flow control within conceptual aircraft design. *Aircraft Engineering and Aerospace Technology: An International Journal (AEAT)* **89**(4), 620–631 (2017)
- [25] Effing, T., Schültke, F., Stumpf, E.: HLFC-optimized retrofit aircraft design of a medium-range reference configuration within the AVACON project. *CEAS Aeronautical Journal* **12**(2), 441–456 (2021)
- [26] Deutsche Aerospace Airbus: Flügel Transporter Masserelevante Daten. Tech. Rep. MA 501 52-01, Luftfahrttechnisches Handbuch, IABG LTH-Koordinierungsstelle, Ottobrunn, Germany (1993)
- [27] Hwang, C.-I., Yoon, K.: Multiple Attribute Decision Making: Methods and Applications A State-of-the-Art Survey. Lecture notes in economics and mathematical systems, vol. 186. Springer, Berlin and Heidelberg (1981)
- [28] Shih, H.-S., Olson, D.L.: TOPSIS and Its Extensions: A Distance-Based MCDM Approach, 1st edn. Springer eBook Collection, vol. 447. Springer International Publishing and Imprint Springer, Cham, Switzerland (2022)
- [29] Jahan, A., Mustapha, F., Sapuan, S.M., Ismail, M.Y., Bahraminasab, M.: A Framework for Weighting of Criteria in Ranking Stage of Material Selection Process. *The International Journal of Advanced Manufacturing Technology* **58**(1-4), 411–420 (2012)
- [30] Zhang, X., Wang, C., Li, E., Xu, C.: Assessment Model of Ecoenvironmental Vulnerability Based on Improved Entropy Weight Method. *The Scientific World Journal* **2014**, 797814 (2014)
- [31] Diakoulaki, D., Mavrotas, G., Papayannakis, L.: Determining objective weights in multiple criteria problems: The critic method. *Computers & Operations Research* **22**(7), 763–770 (1995)
- [32] Dorbath, F.: Large Civil Jet Transport (MTOM > 40t): Statistical Mass Estimation. Tech. Rep. MA 401 12-01, Luftfahrttechnisches Handbuch, IABG LTH-Koordinierungsstelle, Ottobrunn, Germany (2013)
- [33] Horstmann, K.-H.: Ein Mehrfach-Traglinienverfahren und seine Verwendung für Entwurf und Nachrechnung nichtplanarer Flügelanordnungen. Ph.D. thesis, Technische Universität Braunschweig, Braunschweig, Germany (1987)
- [34] Horstmann, K.-H., Engelbrecht, T., Liersch, C.: LIFTING\_LINE: Version 3.0 Revision: User Manual (2019)
- [35] Torenbeek, E.: Advanced Aircraft Design: Conceptual Design, Analysis, and Optimization of Subsonic Civil Airplanes. Aerospace series. Wiley, Chichester (2013)
- [36] Jentys, M., Effing, T., Breitsamter, C., Stumpf, E.: Numerical analyses of a reference wing for combination of hybrid laminar flow control and variable camber. *CEAS Aeronautical Journal* **13**(4), 989–1002 (2022)
- [37] Reckzeh, D.: Multifunctional Wing Moveables: Design of the A350XWB and the Way to Future Concepts. In: Proceedings of the 29th Congress of the International Council of the Aeronautical Sciences, St. Petersburg, Russia (2014)
- [38] Mauerer, P.: Integration of variable camber capabilities into an aerodynamic database driven preliminary wing design methodology. Master thesis, RWTH Aachen University, Aachen, Germany (2023)
- [39] Lange, F.: High Fidelity Design of the AVACON Research Baseline Aircraft based on CPACS Data Set. In: Association Aéronautique et Astronautique de France (ed.) 54th 3AF International Conference on Applied Aerodynamics (2019)